Solidification Modeling: Evolution, Benchmarks, Trends in Handling Turbulence, and Future Directions

SUDEEP VERMA and ANUPAM DEWAN

A systematic evolution of the solidification modeling is presented in this article. An approach starting from the basic governing equations to the intricate modeling of the alloy solidification using different approaches has been reviewed. Important advantages and issues related to different formulations and the use of fixed/moving grids for the modeling of solidification have been discussed. This article outlines the important solidification modeling approaches used in the literature. The mathematical description of the most frequently employed methods for modeling of solidification has been presented providing adequate references for other solidification models. This article highlights an important subdomain of solidification modeling, namely, the modeling of solidification processes having significant turbulence (such as welding, casting, and Czochralski crystal growth). A review of the use of different turbulence models along with the state-of-the-art techniques in these areas is presented. The paper also describes the important benchmarking studies (both experimental and numerical modeling results) used for the validation of solidification of both pure metals and alloys. Finally, the physical and numerical complexities associated with the solidification modeling phenomena along with the important challenges and future directions are presented.

DOI: 10.1007/s11663-014-0039-6

I. INTRODUCTION

SOLIDIFICATION is an important phenomenon in the field of welding, casting, growth of single crystals for electronic and optoelectronic applications and many other industrial and research applications. A prediction of defects, microstructures, residual stresses, *etc*., in the solidified material is indispensible in these processes as these features control the final desirable characteristics, such as strengths of welded joint and cast product and electronic and optoelectronic properties of single crystals.[1] A direct observation and quantification of these features during the course of solidification is possible by highly sophisticated *in situ* observation techniques requiring additional elaborated setups.[2–5] Considering the fact that for the abovementioned solidification processes (welding, casting, and single crystal growth by Czochralski technique) the presence of turbulence also affects these features, and therefore, an *in situ* monitoring setup is required, which has extremely high resolution to capture them in a realistic manner. On the other hand, post-solidification analysis of these features provides an assessment of their values and distribution in the material, but seldom indicates the reasons for their evolution and dissemination—which is very important to gain a meaningful insight into the complex solidification process.

Since these effects are closely coupled with the macroscopic and microscopic heat and mass transfers during the phase-change, a pragmatic way to bridge this gap is a systematic numerical modeling of the solidification phenomenon by solving the coupled fluid flow and heat- transfer equations for a given domain. Before starting a discussion on the techniques for solidification modeling, it is appropriate at this point to highlight the important issues associated with solidification modeling. First is the accurate capture of the moving solid–liquid interface, incorporation of the latent heat released at the moving solid–liquid interface, and accommodating the discontinuities in the properties of the solid and liquid phases across the interface. Further, the presence of heat-and mass-transfer effects—from the microscopic scale (morphological scale) to the macroscopic scale (overall domain scale)—adds significantly to the computational resources during the solidification modeling as the length and time scales in the models have to be chosen in such a way to capture both the microscopic and macroscopic effects. A further complication is the fact that techniques for an accurate solidification modeling of pure metal do not work effectively for an alloy. Finally, incorporation of the effects of turbulence during solidification is an important issue affecting the heat and mass transfers at the micro as well as the macro levels.

The abovementioned facts corroborate that solidification modeling is a specialized research topic which requires a synergistic coupling of different domains of science, engineering, and mathematics. However, solidification modeling is one of the most extensively studied

SUDEEP VERMA, Scientist-D, is with the Solid State Physics Laboratory, Timarpur, Delhi 110054, India, and also Ph.D. Candidate, with the Department of Applied Mechanics, Indian Institute of Technology Delhi, Hauz Khas, New Delhi 110016, India. ANUPAM DEWAN, Professor, is with the Department of Applied Mechanics, Indian Institute of Technology Delhi. Contact e-mail: adewan@am.iitd.ac.in

Manuscript submitted August 31, 2013.
Article published online February 19, 2014.

subjects as confirmed by the vast research literature and excellent review articles.[6–17] spanning across the breadth and depth of this subject including specialized models to predict defects, microstructures, residual stresses, *etc*.,[18–22] The current article attempts to review different approaches to tackle various issues concerned with solidification modeling, highlighting significant contributions made by researchers during the course of the development of solidification modeling with an extensive focus on solidification modeling of processes having significant turbulence.

II. EVOLUTION OF SOLIDIFICATION MODELING

Solidification modeling has a deep-rooted history starting with the study of Nicolas Chvorinov in 1940 on the theory of casting solidification.[23] Chvorinov's rule for calculating the solidification time for a casting, one of the most useful guides in casting, was complemented and substantiated by the pioneering study of Campbell, who himself contributed significantly in providing experimental benchmarks and modeling of defects during casting.[24,25] It was the early study of Eyres *et al*.[26] on the formulation of *Enthalpy method*, which paved the way for the use of numerical methods for modeling solidification. Later key studies of Chalmers[27] and Flemings[28] on heat and solute balance at the solidifying interface added another milestone to the evolution of solidification modeling. Kurz and Fisher[1] in their book on fundamentals of solidification discussed the evolution of solid–liquid interface, single-phase and multiphase solid–liquid interface geometries, the effect of solidification on the redistribution of solute, and the effects of high- and low-growth rates upon microstructure. During the same time period, Crank[29] published his famous book on free and moving boundary problems in which he discussed various front-tracking methods based on the moving and fixed grids.

In addition to the abovementioned studies, the early studies of Szekely,[30,31] Mehrabian *et al*.,[32] Ridder *et al*.,[33] and Hills *et al*.[34] contributed to a great extent in the development of solidification modeling. These important developments facilitated researchers in proposing more specific formulations for modeling solidification. The subsequent significant works along with the essential details of the abovementioned studies have been discussed below.

III. GOVERNING EQUATIONS FOR MODELING SOLIDIFICATION

As applicable to any transport phenomenon, the governing equations for modeling the solidification are the conservation of mass, momentum, energy, and species equations and these may be written as.[35]

Equation for conservation of mass/continuity equation:

$$\frac{\partial \rho}{\partial t} + \mathrm{div}(\rho \mathbf{u}) = 0, \qquad [1]$$

where ρ denotes the density, and $\mathbf{u} = (u,v)$ the velocity.

Equation for conservation of x-momentum:

$$\frac{\partial(\rho u)}{\partial t} + \mathrm{div}(\rho \mathbf{u} u) = \mathrm{div}(\mu \mathrm{grad} u) - \frac{\partial p}{\partial x} + Au, \qquad [2]$$

where μ denotes the viscosity, p the effective pressure, and Au the x-momentum source term.

Equation for conservation of y-momentum:

$$\frac{\partial(\rho v)}{\partial t} + \mathrm{div}(\rho \mathbf{u} v) = \mathrm{div}(\mu \mathrm{grad} v) - \frac{\partial p}{\partial y} + Av + S_b, \qquad [3]$$

where Av denotes the y-momentum source term, and $S_b = \frac{\rho_{\mathrm{ref}} g \beta (h - h_{\mathrm{ref}})}{C}$ is the buoyancy source term assuming the *Boussinesq approximation*.

Equation for conservation of energy:

$$\frac{\partial(\rho h)}{\partial t} + \mathrm{div}(\rho \mathbf{u} h) = \mathrm{div}(\alpha \mathrm{grad} h) + S_h \quad (\text{Enthalpy formulation}), \qquad [4a]$$

where $h = \int_{T_{\mathrm{ref}}}^{T} c \mathrm{d}T$ denotes the sensible enthalpy, $\alpha = k/c$ the thermal diffusivity, and S_h the energy source term.

Alternatively, temperature formulation can also be used for the conservation of energy equation.

$$\frac{\partial(\rho T)}{\partial t} + \mathrm{div}(\rho \mathbf{u} T) = \mathrm{div}(\alpha \mathrm{grad} T) + S_t \quad (\text{temperature formulation}), \qquad [4b]$$

where S_t denotes the energy source term.

Equation for conservation of species:

$$\frac{\partial(\rho m_l)}{\partial t} + \mathrm{div}(\rho \mathbf{u} m_l) = \mathrm{div}(\Gamma_l \mathrm{grad} m_l) + R_l, \qquad [5]$$

where m_l denotes the species mass fraction, Γ_l the species diffusion coefficient, and R_l the species source term.

It is to be noted that Boussinesq approximation is used to introduce buoyancy in the flow. However, its validity is limited to approximately 10 pct of the variations of the thermophysical properties.[36]

The above equations are suitably modified using different formulations for the source terms and effective material properties (formulated as a function of temperature, pressure, *etc*.,) to account for the phase-change phenomenon. For modeling the solidification, the solid and liquid phases (separated by a moving interface) are described by these modified equations which are discretized using different discretization techniques and then solved using numerical methods. Initial solidification models employed the finite difference method (FDM) for the discretization of these governing equations, which later paved way for more sophisticated and accurate discretization methods, such as the finite element method (FEM) and the finite volume method (FVM).

IV. STEFAN PROBLEM

As discussed in Section III, the solid and liquid phases are separated by an interface. The position and shape of

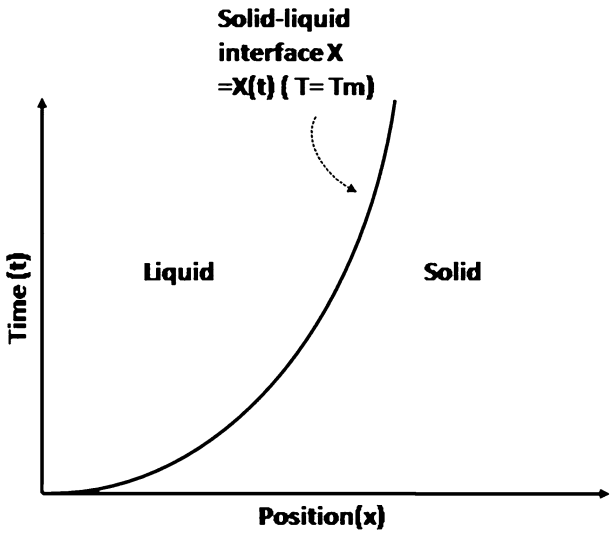

Fig. 1—Evolution of solid–liquid interface for a one dimensional Stefan problem.

the interface in space and time are usually not known initially, but has to be determined as a part of the solution. Such type of moving boundary problems are called as the Stefan problem based on the early study of Stefan.[37,38] In addition to computing the position of interface boundary between the different phases, incorporation of Stefan condition in the model also requires accounting for discontinuities in the thermophysical properties (thermal conductivity, heat capacity, density, *etc*.,) for the solid and liquid phases across the interface boundary. These discontinuities in the thermophysical properties further complicate the numerical solution with the introduction of large discontinuities in the coefficients of the governing differential equations.[11,39] Different methodologies are adopted in the literature to incorporate the Stefan condition, depending on the type of modeling approach (fixed grid/single domain or moving grid/multidomain) and formulation of energy equation (temperature based or enthalpy based).[29,40] Stefan condition is used as energy balance equation at the solid–liquid interface for finding the location and shape of the solid–liquid interface. Stefan condition for a one-dimensional solidification is written as follows:

$$k_s \frac{\partial T_s}{\partial x} - k_l \frac{\partial T_l}{\partial x} = L\rho \frac{\partial X}{\partial t}, \qquad [6]$$

where k_s and k_l are the conductivities of the solid and liquid, respectively; L is the latent heat; $\frac{\partial T_s}{\partial x}$ and $\frac{\partial T_l}{\partial x}$ are the temperature gradients in solid and liquid regions near the interface, respectively; and $\frac{\partial X}{\partial t}$ is the interface movement rate. Figure 1 shows the evolution of the solid–liquid interface for a one-dimensional Stefan problem.

V. APPROACHES FOR MODELING SOLIDIFICATION OF PURE METALS

In the case of pure metals, solidification takes place at a fixed temperature, and hence, the phase-change region consists of the solid and liquid regions separated by a sharp interface as shown in Figure 2.

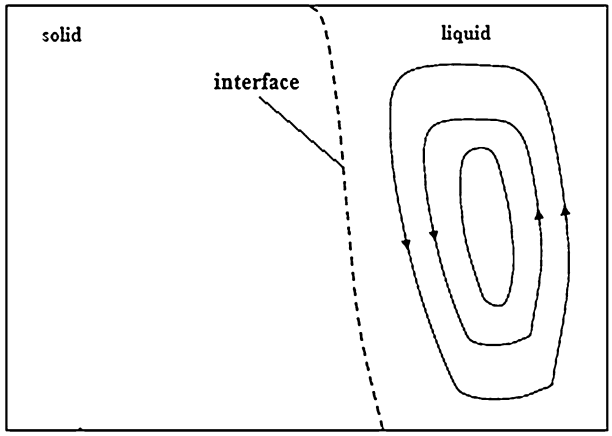

Fig. 2—Phase-change region for solidification of pure metal.

Some of the evolutionary studies on the solidification modeling made use of the semiempirical methods which applied only the conduction treatment and accounted for the convective heat transfer and release of latent heat by equivalent enhancement of the conductivity and the heat capacity.[11,41,42] Szekely *et al*.[30,31] were the first to report the combined effects of convection and diffusion on the solidification of pure lead. The above studies marked the beginning of the development of sophisticated solidification models. Thereafter, there has been a systematic progress in the solidification modeling of pure metals.

A. *Multidomain Approach (Moving Grid Method)*

Starting models for the solidification modeling were mainly based on the multidomain approach.[43–45] This involved solving two different sets of governing equations for each phase. The Stefan condition was used at the solid–liquid interface to calculate the interface velocity, and the interface was moved depending on the velocity at each time step. The updated solid and liquid regions were then meshed again. Figure 3 shows the solid–liquid interface of a two-dimensional solidification domain using a moving grid. The moving grid methods predict sharp interfaces and have good accuracy in the prediction of properties around the interface, and therefore, they are good candidates for the solidification modeling of pure substances which have sharp melting points.[46] Demizdzic and Peric[47,48] have presented a general formulation for solving the conservation equations governing the fluid flow on the moving grids. In the case of moving grids, in addition to the equations for the conservation of mass, momentum, and energy, space conservation needs to be satisfied to avoid the inclusion of artificial mass source (or sink) in the continuity equation. The space conservation law was first proposed by Thomas and Lombard[49] and later formulated in detail by Demizdzic and Peric.[47,48] The formulation of the discretization process for the conservation equations based on the finite volume technique

for the moving grids has been discussed in detail by Ferziger and Peric.[50]

As already mentioned, the moving grid methods are associated with complications of deforming grids (to capture the moving interface) or the coordinate transformation, which contribute significantly to model complexity and computational resources. Further, the use of techniques for accommodating the latent heat/Stefan condition in the energy equation based on temperature formulation with a moving grid method is an intricate job and requires a careful formulation as highlighted by Szimmat[51] who performed a comparison of both the temperature- and enthalpy-based formulations of energy equation for modeling the solidification.

B. *Single Domain Approach (Fixed Grid Method)*

The complexities associated with the multidomain approach motivated researchers to envisage an altogether different approach employing a single computational domain with fixed grids to model both the solid and liquid phases during the solidification. This approach involves tracking the interface by evaluating nodal liquid fraction (f) which takes values $0 \le f \le 1$. The *Enthalpy method* as proposed by Eyres *et al.*[26] and later by Price and Slack[52] emerges as the obvious choice for the formulation of energy equation in the fixed grid domain as it avoided nonlinearity in the energy equation without incorporating additional dynamic thermal condition on the solidification front on a fixed grid. Figure 4 shows the solid–liquid interface of a two-dimensional solidification domain using fixed grid.

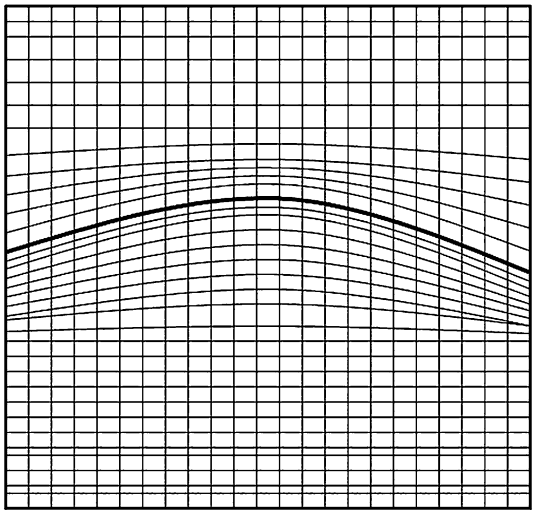

Fig. 3—Moving grid (dark line shows the solid–liquid interface).

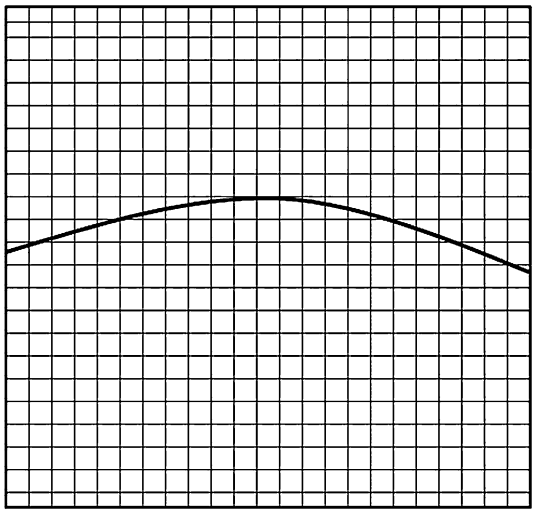

Fig. 4—Fixed grid (dark line shows the solid–liquid interface).

1. *The Enthalpy–Porosity Approach Based on Fixed Grid Method*

Voller and Cross[53] further refined the enthalpy method for accurate solutions of the moving boundary problems and later Voller *et al.*[54–56] supplemented it by adding the porous formulation for the phase-change region to give rise to the famous *enthalpy–porosity approach*. In the *enthalpy–porosity approach*, the need for the incorporation of the Stefan condition into the single domain is achieved by adopting enthalpy formulation for the energy equation instead of the temperature formulation. This formulation incorporates the latent heat by including a temperature-dependent latent heat source term (S_h) in the energy equation.

For the case of solidification of a pure metal, the liquid- to solid-phase change occurs isothermally, and the mean nodal latent heat (ΔH) is defined as[57,58]

$$\begin{matrix} \Delta H = f(T) = L & T > T_{\mathrm{m}} \\ 0 & T < T_{\mathrm{m}} \end{matrix}, \qquad [7]$$

where L denotes the latent heat of fusion, and T_{m} the melting point of the pure substance. Hence, no explicit condition on the heat flow at the solid–liquid interface is required.

However, the simplification due to single domain using fixed grid posed another challenge of accommodating the zero velocity in that part of the domain that turns into solid from liquid during the course of solidification. Several methods have been proposed by different researchers to "switch off" the velocity in the computational cells which are solidifying. Morgan[59] employed a simple approach of making the velocities zero in the computational cells mean latent heat content (ΔH) of which reaches some set value [between 0 (fully solid) and L (fully liquid), where L denotes the latent heat of phase change]. Gartling[60] employed a more refined approach of increasing the viscosity of the computational cells to a very large value mean latent heat content of which reduces to zero. This approach provides a kind of realistic coupling between the physical state of the material in the computational domain and the corresponding momentum equations. Voller *et al.*[54–56,58] after investigating various velocity-switching methods proposed an approach in which the computational cells undergoing phase change are modeled as pseudo porous media porosity of which reduces from 100 pct in the liquid domain to 0 pct in the solid

domain. This behavior is achieved by introducing source terms (Au and Av in Eqs. [2] and [3]) in the momentum equations which model the interface region as porous media with a suitably defined permeability,[61,62] and hence, this technique was named the *enthalpy–porosity technique* (as it uses the enthalpy formulation for the energy equation and models the interface region as porous media for gradually extinguishing the velocities from the liquid to the solid regions).

The enthalpy–porosity method uses the same general conservation equations as described in Section III (Eqs. [1] through [5]).

To account for the latent heat, the energy source term (S_h) in Eq. [4a] is defined as

$$S_h = \frac{\partial(\rho \Delta H)}{\partial t} + \mathrm{div}(\rho \mathbf{u} \Delta H). \qquad [8]$$

In the case of an isothermal phase change, the second term describing the convective part of the source term ($\mathrm{div}(\rho \mathbf{u} \Delta H)$) is zero because of the zero velocity at the solid–liquid interface and ΔH is a temperature-dependent function as defined in Eq. [7]. Voller and Prakash[58] and Swaminathan and Voller[63,64] have provided reliable methods for updating the latent heat content of each computational cell according to the predicted temperature value after each iteration.

Voller *et al.*[65] have reviewed other fixed grid techniques for modeling the phase change which can also be suitably applied to model the solidification.

It is seen that the fixed grid methods offer considerable computational convenience; however, these pose challenges to a programmer in accommodating sharp discontinuities in the material properties across the thin interface during the solidification modeling of pure metals. Further several constraints need to be exercised in the formulation of momentum source terms (Au and Av) for extinguishing velocities smoothly from the liquid to solid regions to ensure that the method chosen allows a smooth, gradual transition rather than a step change in the velocity. Since step changes in the momentum equation, source terms tend to retard the convergence of the numerical solution and may lead to oscillations. This problem can be avoided by employing a numerical fix of associating some finite width to the solid–liquid interface (which ideally should be a well-defined line) so that velocities are gradually reduced to zero and step changes in velocities are avoided.

Hence, for pure metals, the fixed grid methods are less efficient in tracking the solid–liquid interface explicitly and accurately compared with the moving grid methods.

VI. APPROACHES FOR MODELING SOLIDIFICATION OF ALLOYS

In contrast to the isothermal solidification of a pure metal, the solidification in case of alloys takes place over a finite temperature range and the computational domain is divided into three regions, namely, liquid, mushy zone, and the solid regions as shown in Figure 5.

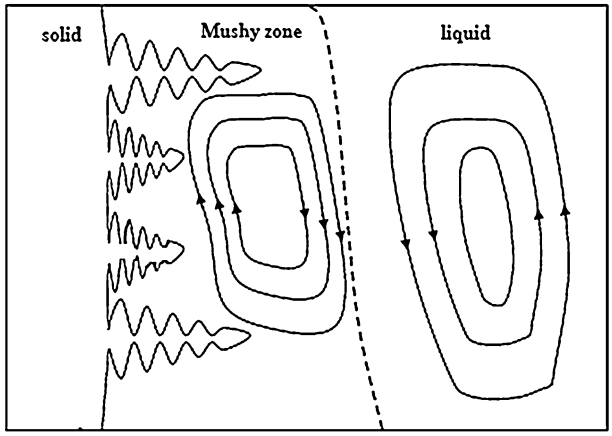

Fig. 5—Phase change region in case of alloy solidification.

The modeling of alloy solidification marks its origin with the study of Flemings *et al.*[66–68] They modeled the mushy zone during the alloy solidification as a porous medium and calculated the macrosegregation. Later Mehrabian *et al.*[32] incorporated the effect of gravity and used Darcy's law to model the flow in porous mushy zone. Szekely and Jassal[69] contributed by providing the solution procedure for the energy equation in the mushy zone, whereas Fuji *et al.*[70] contributed by providing solution procedure for the coupled mass, momentum, energy and species equations in the mushy zone only without considering the convection in the pure liquid region. However, Ridder *et al.*[33] were the first to solve the complete set of conservation equations for both the mushy and pure liquid zones. Since different sets of equations were used for the mushy and liquid regions, these researchers used the multidomain approach to model the solidification.

As discussed in the case of solidifications of pure metals in Section V, fixed grid/single domain methods handle interface with finite width (mushy zone in case of alloy solidification) in an easy and straightforward manner compared with the moving grid/multidomain methods, and considering the computational convenience offered by the fixed grid methods, developments of models based on the single-domain approach/fixed grid for modelling the alloy solidification also started along with the multidomain approach. Single-domain methods as proposed by Prantil and Dawson[71] and Hills *et al.*[34] were some of the initial models for modeling the alloy solidification.

Before discussing different approaches for modeling alloy solidification, it is important to discuss the role of *double-diffusive convection* in alloy solidification. The double-diffusive convection also called as the thermosolutal convection is the fluid flow generated by the buoyancy effects because of both the temperature and concentration gradients. This phenomenon exhibits a no. of surprising effects and complex flow structures when molecular diffusivities are different for the thermal and solutal gradients acting in the opposite directions.[72–75] As a result, convective layers which are solutally well mixed but are separated by thin interfaces

with a step-like density distribution are observed. This causes considerable variations in the local melting rate, the interfacial temperature, and the concentration distribution.[76,77] The double-diffusive convection is an important characteristic of the alloy solidification which makes the overall modeling of alloy solidification a complicated task.

As in the case of solidification of pure metals, the modeling approaches for alloy solidification can also be classified as those based on the fixed grid or the moving grid techniques. However in the case of alloy solidification, the most important criterion depends on the way the microscopic heat and mass transfers are handled. Based on this criterion, two important approaches for modeling the alloy solidification have been reported in the literature. The first approach is based on the classical mixture theory proposed by Bennon and Incropera,[78,79] and the second approach is based on the volume-averaging technique proposed by Beckermann and Viskanta[75] and later modified by Ni and Beckermann.[80] These two approaches have been discussed in detail later.

A. *Modeling Approach for Alloy Solidification Based on Classical Mixture Theory*

Benon and Incropera developed a continuum-based binary alloy solidification model with a consistent set of conservation equations for the mass, momentum, energy, and species. They incorporated the mixture theory[81–85] based on the assumptions of mixture components treated as isolated subsystems with the mixture properties and behavior governed by the component properties and governing equations of individual components. The conservation equations associated with phase k in a multiphase mixture as proposed by them are[78]

Equation for conservation of mass:

$$\frac{\partial(\rho)}{\partial t} + \nabla.(\rho \mathbf{V}) = 0, \qquad [9]$$

where $\rho = \sum_k \bar{\rho}_k$ denotes the mixture density with $\bar{\rho}_k = g_k \rho_k$; g_k and ρ_k denote the actual density and volume fraction of the phase k, respectively, $\mathbf{V} = \frac{1}{\rho}\sum_k \bar{\rho}_k \mathbf{V}_k = \sum_k f_k \mathbf{V}_k$; $\mathbf{V}_k$ denotes the phase velocity and $f_k = \frac{\bar{\rho}_k}{\sum_k \bar{\rho}_k}$ the mass fraction of phase k.

Equation for conservation of x-momentum:

$$\begin{aligned}\frac{\partial(\rho u)}{\partial t} + \nabla.(\rho \mathbf{V} u) &= \nabla.\left(\sum_k g_k \tau_{kx}\right) \\ &\quad - \nabla.\left(\sum_k \bar{\rho}_k (\mathbf{V}_\mathbf{k} - \mathbf{V})(u_k - u)\right) \\ &\quad - \frac{\partial\left(\sum_k g_k p_k\right)}{\partial x} + \rho B_x + F_x,\end{aligned} \qquad [10]$$

where $u = \frac{1}{\rho}\sum_k \bar{\rho}_k u_k$; u_k denotes the x-component of the velocity of phase k; τ_{kx} is the phase stress vector which includes the stresses resulting from the interactions of a phase with itself; p_k is the pressure force of phase k; $B_x = \frac{1}{\rho}\sum_k \bar{\rho}_k B_{kx} = \sum_k f_k B_{kx}$; B_{kx} denotes the x-component of the body force on the phase k, and F_x the net force in the x-direction due to the interaction between phases. Conservation equation for the y-momentum can be written in a similar manner.

Equation for conservation of energy:

$$\begin{aligned}\frac{\partial(\rho h)}{\partial t} + \nabla\cdot(\rho \mathbf{V} h) &= \nabla\cdot\left(\frac{k}{c_k}\nabla h\right) + \nabla\cdot\left(\frac{k}{c_k}\nabla(h_k - h)\right) \\ &\quad - \nabla\cdot\left(\sum_k \bar{\rho}_k(\mathbf{V}_\mathbf{k} - \mathbf{V})\right)(h_k - h)\end{aligned} \qquad [11]$$

where $h = \frac{1}{\rho}\sum_k \bar{\rho}_k h_k = \sum_k f_k h_k$ denotes the mixture enthalpy; h_k denotes the enthalpy of the phase k; $\mathbf{k} =_k g_k k_k$ denotes the mixture conductivity; $\mathbf{k}_k$ is the conductivity of phase k; and c_k is the effective specific heat of phase k.

Equation for conservation of species:

$$\begin{aligned}\frac{\partial(\rho f^\alpha)}{\partial t} + \nabla\cdot(\rho \mathbf{V} f^\alpha) &= \nabla\cdot\left(\sum_k \rho f_k D_k^\alpha \nabla f_k^\alpha\right) \\ &\quad - \nabla\cdot\left(\sum_k \bar{\rho}_k(\mathbf{V}_\mathbf{k} - \mathbf{V})(f_k^\alpha - f^\alpha)\right),\end{aligned} \qquad [12]$$

where $f^\alpha = \frac{1}{\rho}\sum_k \bar{\rho}_k f_k^\alpha = \sum_k f_k f_k^\alpha$ denotes the mixture concentration of species α; $f_k^\alpha = \frac{\bar{\rho}_k^\alpha}{\bar{\rho}_k}$ denotes the mass fraction of the constituent α in the phase k, and $\bar{\rho}_k^\alpha = g_k^\alpha \rho_k^\alpha$; ρ_k^α and g_k^α denote the actual density and the volume fraction of constituent α in the phase k, respectively; f_k denotes the mass fraction of species α; and D_k^α is the diffusion coefficient of species α in phase k.

Benon and Incropera[78,79] further simplified these equations for the case of two-phase, solid–liquid system for modeling the binary alloy solidification. In this model, supplementary relations, required to find the values of the mass fraction f_k and the composition f_k^α to close the system of equations, are formulated assuming the local composition equilibrium at phase interfaces which allows coupling of continuum and phase compositions with temperature through equilibrium phase diagram using the lever rule. However, Voller *et al.*[86] have emphasized that such temperature–solute coupling based on the lever rule under the assumption of thermodynamic equilibrium is valid only when the solid phase is dispersed into the liquid in the mushy zone, and they highlighted the need for nonequilibrium temperature–composition coupling (Scheil equation) when the mushy zone has a distinct microstructure which is shown in Figure 6.

B. *Modeling Approach for Alloy Solidification Based on Volume Averaging of Microscopic Transport Equations*

It is evident from Section VI–A that the modeling of alloy solidification using the continuum approach based on the mixture theory offers several advantages in terms of easier formulation and computational convenience. However, this type of formulation is restricted to model the macroscopic (~10^{-2} m) transport properties only, such as pressure, velocity of fluid, temperature, concentration, and volume fraction providing information

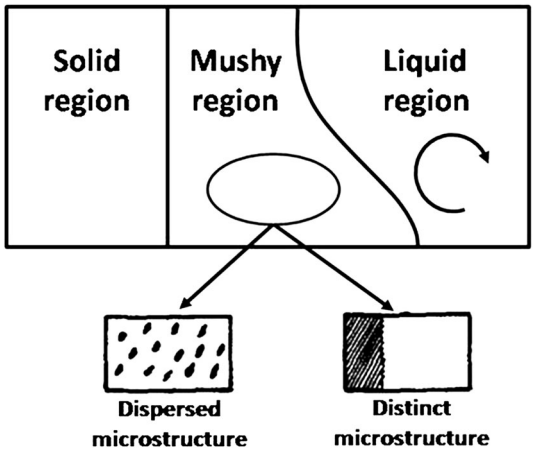

Fig. 6—Dispersed and distinct microstructures in case of alloy solidification.

about the convective flow pattern, heat flux through different boundaries, and macrosegregation. However, information about the important microscopic (~10^{-4} to 10^{-5} m) properties, such as microsegregation, grain size, morphology in the mushy zone, orientation, porosity, *etc*., is not deciphered with this approach.[87] Reducing the modeling length and time scales to incorporate these microscopic phenomenon is impractical even with the current computational resources, as it is usually impossible to solve the exact conservation equations on a microscopic scale because of the complex interfacial structure present in a multicomponent solidification. A practical solution to this problem is to solve the macroscopic and microscopic models separately and provide a suitable coupling between these models to simulate the interactions at different scales. Rappaz[6] has reviewed a no. of models for the micro-macro coupling and the prediction of microstructure. An appropriate coupling approach is to average out the microscopic equations over a finite size volume (containing both solid and liquid) to get the macroscopic equations. Drew[7,88] has described a no. of averaging techniques which can be suitably used to derive the macroscopic equations from the microscopic equations. Since the mushy zone is mainly composed of relatively stationary and geometrically complex solid structures, volume-averaging approach[89–93] is the most commonly used technique.

The use of the volume-averaging technique was first proposed by Beckermann and Viskanta.[75] They developed a single set of volume-averaged macroscopic equations which are valid in all the three zones (solid, liquid, and the mushy) using the continuum approach considering stationary columnar dendritic mushy zone for modeling the binary alloy solidification. However, the model had considerable uncertainty in the prediction of the structure, permeability, and anisotropy of the mushy zone. The model did not have any means to predict the nonstationary solid phase (dispersed phase), and further more it did not resolve the strong gradients associated with the double-diffusive interface. Ganesan and Poirer[94] used the similar approach to derive the mass and momentum equations for the flow through a stationary dendritic mushy zone with more general forms of momentum equations.[94]

A further extension to the use of volume-averaging method was done by Prakash[95,96] and Ni and Beckermann[80] employing the two-phase model in which separate volume-averaged conservation equations for the mass, momentum, species, and energy were solved for the solid and liquid phases. While the model proposed by Prakash[95,96] had a provision of actually computing the motion of the dispersed solid phase, the model by Ni and Beckermann[80] included the solute undercooling effect along with computing the moving solid fractions. Their model did not assume complete solid and liquid equilibrium and therefore accounted for the solute undercooling which helps in predicting the microstructure and strong gradients associated with the double-diffusive convection.

Prescott *et al*.[97] performed a comparison of the continuum approach based on the mixture theory and volume-averaging approach for modeling the binary alloy solidification and showed that a careful formulation yields the same macroscopic equations with both the approaches. A comparison between the benefits and shortcomings of the continuum and two-phase approaches for modeling the binary alloy solidification was performed by Ni and Incropera[98,99] who further extended the basic continuum single-phase model for the solidification based on the mixture theory proposed by Bennon and Incropera.[78,79] They started with the two-phase formulations as proposed by Ni and Beckermann[80] and derived a single set of conservation equations. This model mostly resolved the modeling of solutal undercooling, solid movement, and established coupling between the micro-macro-level phenomena retaining the numerical convenience of the single-phase continuum approach.

Later Reddy and Beckermann[100] also employed a simplified version of the two-phase model of Ni and Beckermann[80] to study the effect of thermosolutal buoyancy and contraction-driven mushy zone flows on macrosegregation in DC continuous casting of an Al-Cu round ingot, which on comparison with the corresponding experimental results showed that the model was able to predict the important macrosegregational features.

The above discussion highlights the aspects related to binary alloy solidification. It is Krane *et al*.[101,102] who extended the continuum mixture theory for the modeling of ternary alloy solidification and later in developing models for predicting microsegregation in ternary alloy solidification.[103] They also performed pioneering work in providing the benchmarking experimental information for validating the developed models for alloy solidification.[104,105]

VII. SOLIDIFICATION MODELING OF PROCESSES WITH TURBULENCE

So far we have seen the approaches for the solidification modeling assuming laminar-flow behavior; however, for the processes considered in this section [welding,

casting and Czochralski (CZ) crystal growth] turbulence plays an important role along with other transport mechanics. Transition from laminar-to-turbulent flow significantly alters the heat-flow and mass-transfer characteristics thereby affecting the movement of the solidification interface and its associated thermal gradients during the phase change and hence controlling the microstructure and solute distribution in the final solidified material.

Turbulence effects in solidification modeling are usually incorporated by suitable modifications of the governing equations in the Reynolds–Averaged Navier–Stokes (RANS)-based turbulent models,[106] but lately, the use of large eddy simulation (LES)[106] is emerging. However, direct numerical simulation (DNS)[106] is still limited to idealized cases and simple geometries due to the complex and coupled nature of the problem. The evolution of turbulent modeling along with the state-of-the-art technique for the above mentioned three processes is discussed later.

A. *Solidification Modeling of Welding Process*

Welding is an important process wherein the melt convection and heat and mass transports in the small weld pool are strongly influenced by the buoyancy, electromagnetic, and surface tension forces. The presence of large thermal and solutal gradients in the weld pool both spatially and temporally make the flow turbulent in nature. Hence, the accuracy of numerical solution in welding is dependent on the accuracy of turbulent models governed by strong buoyancy, electromagnetic, and surface tension forces. Incorporation of the turbulence effects in the modeling of solidification process during the welding was first done by Zacharia *et al.*[107] They made use of a simple subelement-scale turbulence model to simulate large-scale convection eddies that form in the melt pool in a moving gas tungsten arc-welding (GTAW) process including the effect of surface tension influencing the melt pool height and the Marangoni convection governed by surface temperature gradient. Later, Mundra *et al.*[108] made use of the enhanced molten metal viscosity to emulate turbulent momentum transport in the weld pool during the welding of similar metals. Choo and Szekely[109] compared the results of laminar model, enhanced effective viscosity model, and the k–ε turbulence model—incorporating the surface tension effects—-with the experimentally measured weld pool shape in the GTAW pool. Although they employed the standard k–ε turbulence model, wall treatment at the phase boundary was not considered in their study. Nevertheless, it substantiated the turbulent nature of the weld pool and brought out the superiority of the standard k–ε turbulence model in providing a much more realistic weld pool shape in comparison with the enhanced effective viscosity model.

It was Chakraborty *et al.*[110] who developed a comprehensive 2D model capable of predicting the turbulent weld pool convection with phase change along with computing the morphology of the solid–liquid interface using a modified k–ε turbulence model with near wall treatment in an GTAW pool. They assumed the melt surface to be flat with a linear dependence of the surface tension on temperature to simplify the coupling between the surface tension-driven flows and the free-shear viscous flow which redistributes the fluid momentum, energy, turbulent kinetic energy and the dissipation of the turbulent kinetic energy inside the weld pool. The phase-change aspect was implemented by a modified enthalpy–porosity technique. They later extended their study by developing a complete 3D model for the turbulent weld pool convection for the GTAW process.[111] Later, Chakraborty and Chakraborty[112] developed a similar model for studying the turbulent molten pool convection in the case of laser welding of Cu-Ni dissimilar couple. In their study, the prediction of the solutal concentration distribution was in good agreement with the corresponding experimental results. Abderrazak *et al.*[113] also applied the standard k–ε model for modeling CO_2 laser welding of magnesium alloys. Chakraborty[114] further extended the study of Chakraborty and Chakraborty***[112] by modeling the turbulent heat, mass, momentum, and species transports in a molten pool during the melting and solidification in a continuous- conduction-mode laser welding of Cu-Ni dissimilar couple. The predicted results for temperature, velocity and species distributions were found to be in good agreement with the corresponding experimental results.

It is obvious from the above discussion that the modeling of solidification phenomenon in processes—where the momentum, energy, and mass transfer are strongly influenced by surface tension forces and the electromagnetic forces coupled with the viscous forces—is a daunting task. This is confirmed by the fact that almost all the research studies have has employed considerable simplifications, such as neglecting weld surface deformation/curvature, because of surface tension forces, assuming linear dependence of surface tension on temperature, *etc.*, and most importantly employing the standard k–ε model for incorporating turbulence. To the best of the authors knowledge, it is Chatterjee and Chakraborty[115] who have reported the use of LES for modeling laser-induced surface tension-driven flow. They employed a subgrid scale kinetic energy equation along with suitable modeling of the eddy viscosity, production, dissipation, and the total enthalpy for the subgrid closure. They demonstrated that LES predictions are much more consistent and successful in capturing the experimental trends in comparison with those by the standard k–ε model.

B. *Solidification Modeling of Casting Process*

Solidification modeling in casting incorporating turbulence started with the early study of Asai and Szekely[116] who used the Kolmogrov–Prandtl model for the two-dimensional modeling of continuous billet casting. Shyy *et al.*[117] incorporated turbulence effects in the solidification modeling of Ti-6Al-4V alloy using a linear relationship between the eddy and molecular values of viscosity and thermal conductivity.

Murthy *et al.*[118] employed three turbulence models (two models were variants of the standard k–ε model,[106,119] and the third model was the mixing-length-type model) to predict the velocity and turbulent parameters in a heated liquid metal system. Thomas *et al.*[120] studied turbulent, steady-state heat transfer and fluid flow in a continuous slab casting. Later, Flint,[121] Huang *et al.*,[122] and Li[123] reported the use of the standard k–ε turbulence model to solidification in different metallurgical systems. All of them utilized the near-wall functions to damp the turbulence near the wall. However, the implementation of the wall function at the solid–liquid interface is rather complicated as the location of the interface is not known beforehand, and it continuously changes during the course of solidification.

Alternatively, Shyy *et al.*[124] first utilized the low-*Re* k–ε model[106] to predict the phase-change and convection diffusion characteristics during the titanium alloy ingot casting in an electron beam melting process. As the low-*Re* version of the k–ε model does not require any wall functions, it was comparatively simpler to use it in the case of turbulent solidification. Hence, Farouk *et al.*,[125] Murakami,[126] Aboutalebi *et al.*,[127] Seyedein and Hasan,[128] and Guthrie and Tavares[129] have subsequently used the low-*Re* version of the k–ε model for the numerical simulation of different casting systems. Netto and Guthrie[130] developed a comprehensive 3D model for predicting the heat transfer, fluid flow, and solidification of a novel delivery system for a single belt steel casting process using a low-*Re* k–ε model. For the solidification modeling, they used the *enthalpy–porosity scheme* with suitable source terms to model the mushy zone.

Chakraborty *et al.*[131] developed a 2D unsteady model with coupled momentum, heat and species transports including the effect of natural convection. In their model turbulence was accounted for by the standard k–ε model suitably modified to account for the phase change. They included the effect of nonequilibrium solidification and microscale transport in the temperature and solute coupling for precisely estimating the release of the latent heat between the solidus and liquidus temperatures for a binary mixture of NH_4Cl-H_2O solution. They employed a single-phase formulation using fixed grids. Their model was based on a modified *enthalpy–porosity technique,* and the modeling of species transport was carried out using the mixture theory.[78] The conservation equations describing the solidification with turbulence used by them are[131] as follows:

Equation for conservation of mass (continuity equation):

$$\frac{\partial \bar{U}_i}{\partial x_i} = 0, \quad \frac{\partial u_i'}{\partial x_i} = 0, \qquad [13]$$

where $\bar{U}_i$ and u_i' denote the mean and fluctuating components of the velocity, respectively.

Equation for conservation of momentum:

$$\frac{\partial(\rho \bar{U}_i)}{\partial t} + \frac{\partial \rho(\bar{U}_i \bar{U}_j)}{\partial x_j} = -\frac{\partial p}{\partial x_i} + \frac{\partial}{\partial x_j}\left(\mu \frac{\partial \bar{U}_i}{\partial x_j}\right) - \frac{\partial(\rho \overline{u_i' u_j'})}{\partial x_j} + \rho g_i[\beta_T(\bar{T} - T_{\text{ref}}) + \beta_S(C_l - C_{\text{ref}})] - A\bar{U}_i. \qquad [14]$$

Equation for conservation of energy:

$$\frac{\partial(\rho \bar{T})}{\partial t} + \frac{\partial(\rho \bar{U}_i \bar{T})}{\partial x_i} = \frac{\partial}{\partial x_i}\left(\left\{\frac{f_l k_{T_l}}{c_l} + (1 - f_l)\frac{k_{T_s}}{c_s}\right\}\frac{\partial \bar{T}}{\partial x_i}\right) - \frac{1}{c}\frac{\partial(\rho \Delta H)}{\partial t} - \frac{1}{c}\frac{\partial}{\partial x_i}(\bar{U}_i \Delta H) - \frac{\partial(\rho \overline{u_i' T'})}{\partial x_i} \qquad [15]$$

Equation for conservation of species:

$$\frac{\partial(\rho \bar{C}_l)}{\partial t} + \frac{\partial \rho(\bar{U}_i \bar{C}_l)}{\partial x_i} = \frac{\partial}{\partial x_i}\left(\rho_l f_l D_l \frac{\partial \bar{C}_l}{\partial x_i}\right) - \frac{\partial(\rho \overline{u_i' C_{l_i}'})}{\partial x_i} + \frac{\partial}{\partial t}(\rho f_s \bar{C}_l) - k_p \bar{C}_l \frac{\partial}{\partial t}(\rho f_s) \qquad [16]$$

Equations for k and ε:

$$\frac{\partial(\rho k)}{\partial t} + \bar{U}_i \frac{\partial(\rho k)}{\partial x_i} = \frac{\partial}{\partial x_i}\left[\left(\mu + \frac{\mu_t}{\sigma_k}\right)\frac{\partial k}{\partial x_i}\right] + \left[\mu_t\left(\frac{\partial \bar{U}_i}{\partial x_j} + \frac{\partial \bar{U}_j}{\partial x_i}\right)\frac{\partial \bar{U}_i}{\partial x_j}\frac{\varepsilon}{k} - g\beta_T \frac{\mu_t}{\sigma_t}\frac{\partial \bar{T}}{\partial y}\frac{\varepsilon}{k} - g\beta_s \frac{\mu_t}{\sigma_c}\frac{\partial \bar{C}_l}{\partial y}\right] - \rho\varepsilon \qquad [17]$$

$$\frac{\partial(\rho \varepsilon)}{\partial t} + \bar{U}_i \frac{\partial(\rho \varepsilon)}{\partial x_i} = \frac{\partial}{\partial x_i}\left[\left(\mu + \frac{\mu_t}{\sigma_\varepsilon}\right)\frac{\partial \varepsilon}{\partial x_i}\right] + \frac{C_{\varepsilon 1}\varepsilon}{k}\left[\mu_t\left(\frac{\partial \bar{U}_i}{\partial x_j} + \frac{\partial \bar{U}_j}{\partial x_i}\right)\frac{\partial \bar{U}_i}{\partial x_j}\frac{\varepsilon}{k} - g\beta_T \frac{\mu_t}{\sigma_t}\frac{\partial \bar{T}}{\partial y}\frac{\varepsilon}{k} - g\beta_s \frac{\mu_t}{\sigma_c}\frac{\partial \bar{C}_l}{\partial y}\right] - \rho C_{\varepsilon 2}\frac{\varepsilon^2}{k} \qquad [18]$$

The values of various model constants used by them are

$$\sigma_t = 0.9,\ \sigma_c = 0.9,\ \sigma_k = 1.0,\ \sigma_\varepsilon = 1.3,$$
$$C_{\varepsilon 1} = 1.44, \quad \text{and} \quad C_{\varepsilon 2} = 1.92.$$

For the flow modeling in the mushy zone, they used a hybrid approach for the momentum source terms ($A\bar{U}_i$) based on the liquid fraction (f_l) in the mushy zone. For $f_l < 0.5$, a porous formulation based on Darcy's law for modeling the momentum source terms was used, and for $f_l > 0.5$, an enhanced effective viscosity formulation for modeling the momentum source terms was used.

The modeling of the Reynolds stress terms $\left(-\rho \overline{u_i' u_j'}\right)$ was carried out using the extended Bousinessq approximation.[106] The turbulent heat fluxes $\left(-\rho \overline{u_i' T'}\right)$ and the turbulent mass fluxes $\left(-\rho \overline{u_i' C_l'}\right)$ were modeled as

$$-\rho \overline{u_i' T'} = \rho \alpha_t \frac{\partial \bar{T}}{\partial x_i}$$

where α_t is the eddy thermal diffusivity defined as $\alpha_t = \frac{\mu_t}{\rho \sigma_t}$; and $\sigma_t = 0.9$ is the turbulent Prandtl number.

$$-\rho\overline{u_i' C_l'} = \rho D_t \frac{\partial \bar{C}_l}{\partial x_i}$$

where D_t is the eddy mass diffusivity defined as $D_t = \frac{\mu_t}{\rho \sigma_c}$; and $\sigma_c = 0.9$ is the turbulent Schmidt number.

The model predictions in terms of the evolution of the flow with time, the height of the solidified layer, and the evolution of temperature at a particular location were found to be in good agreement with the corresponding experimental results obtained by the authors of the study.[131]

It is clear that most modeling studies on the casting solidification incorporating turbulence have made use of the RANS-based turbulence models. Studies using LES for modeling casting solidification are handful, and the one-equation k-models for modeling the subgrid scales in the filtered Navier–Stokes equations were mostly used in such studies.[132–134] The use of the Smagorinsky eddy viscosity model[135] and the wall-adapting large eddy-viscosity (WALE) model[136] have also been reported for modeling the subgrid scales. For details about the formulations of various subgrid models, the reader is referred to an excellent book by Sagaut.[137]

C. *Solidification Modeling of Czochralski Crystal Growth Process*

Of different techniques to grow bulk crystals from melt,[138] Czochralski (CZ) technique or crystal pulling stands out to be the most preferred one offering large diameter, high growth rates with good crystalline quality, and hence is commercially the most commonly used technique for the large-scale growth of various semiconductor and oxide crystals. However, the complex nature of flow makes solidification modeling difficult in this process. Melt convection in Czochralski growth process is an outcome of a no. of factors (buoyancy, Coriolis, centrifugal, surface tension, and forced convection due to crystal-crucible rotation) and possesses a no. of flow instabilities.[139] Owing to these factors which occur at different length and time scales, the flow in the Czochralski process is turbulent in nature.

The incorporation of turbulence effects in CZ modeling started in the early 1990s with the study of Kobayashi *et al.*[140] who performed analytic studies using the k–ε model to carry out heat-transfer analysis in Si-CZ setup. Later, Ristorcelli and Lumely[141] used the Reynolds stress transport model (RSM) to carry out simulation of buoyancy-driven flow in the CZ melt. Assaker *et al.*[142] utilized the mixing-length model for predicting the melt convection in the CZ setup. Lipchin and Brown[143] performed a comparison of three turbulence models (the standard k–ε model with the wall functions, k–ε model with one equation model for the flow near walls, and a low-*Re* k–ε model) to predict the flow, temperature fields, and oxygen transport in a prototype model of the CZ setup. They showed that in highly turbulent regime the predictions of all the three models were almost similar in nature. However, in the near-wall region, where turbulence is weak and viscous forces dominate, only the low-*Re* k–ε model provided satisfactory results.

Basu *et al.*[144] carried out complete 3D, unsteady, turbulent flow, and heat-transfer analysis of the melt in the CZ crystal growth process using the block-structured grid for the first time using a quasi DNS.[145] On similar lines, Enger *et al.*[146] and Vizman *et al.*[147] carried out comparison of the measured and predicted temperature fields in an industrial Si-CZ melt during the real crystal growth conditions. Vizman *et al.*[148] even extended their work by comparing the 3D numerical results with temperature distributions measured in Si-CZ melts under the influence of different magnetic fields. They also highlighted the suitability of 3D time dependent simulations for predicting the measured temperature distribution in comparison to 2D computations using the standard k-ε model.

Evstratov *et al.*[149] performed 3D modeling of turbulent melt convection using a hybridization of Reynolds-averaged approach and LES. They employed an unsteady RANS treatment in the near-wall region and LES with standard Smagorinsky subgrid scale model in the flow core to study the effect of the suppression of turbulent melt convection under the effect of magnetic field in a Si-CZ system. Ivanov *et al.*[150] performed a similar study using a RANS/LES hybridization model for turbulence. Kalaev *et al.*[151] studied the effect of inert gas flow on the global heat exchange, turbulent melt convection, and deflection in the interface for different gas flow rates in an industrial CZ-Si growth system. They used a modified low-*Re* k–ε model for the turbulent melt convection. Krauze *et al.*[152] carried out the 3-D melt flow structure analysis in the presence of horizontal DC magnetic field using the RNG k–ε model. Wagner and Friedrich[153] performed DNS to investigate the effect of crystal and crucible rotation on the flow structure and temperature fluctuations in an idealized CZ melt.

Smirnova *et al.*[154] performed LES of CZ growth and studied the effect of crucible rotation rates on the crystallization rate of $Si_{1-x}Ge_x$ crystals. Son *et al.*[155] studied the effect of co- and counter-rotation of crystal-crucible on the thermal and velocity fields in the CZ system using the k–ε turbulent model. Roufeisen *et al.*[156] performed a DNS for a turbulent rotating buoyancy and surface tension-driven flow in an idealized CZ configuration and later they validated the LES data[157] with the same configuration using both the standard Smagorinsky and dynamic subgrid scale models for different discretization schemes and showed that computational effort can be significantly reduced using LES. They suggested that extreme care should be taken for the grid resolution and choice of discretization scheme for the convective terms. Later, they performed LES including the variations in the diameter of the growing crystal[158] and then extended it for LES[159] for a transient 3D turbulent melt flow and heat transfer simultaneously predicting the phase interface, moving free surface including meniscus and the three-phase boundary between the melt, crystal, and the surrounding atmosphere. For both these studies, they employed the standard Smagorinsky subgrid scale model using the dynamic procedure of Germano *et al.*[160]

Noghabi *et al.*[161] studied the effect of crystal and crucible rotation rates on the shape of the interface during the Si-CZ growth employing a 2D axisymmetric

model based on one-equation turbulent RANS approach. Miller *et al.*[162] carried out local 3D melt flow analysis for the CZ growth of square-shaped Si crystals under travelling magnetic field. They employed a two-level approach. In the first level they calculated the temperature field boundary conditions for the crucible outer walls, solid–liquid interface and free melt surface and also the Lorentz force on the crucible melt using the commercial software CrysMAS. In the second level, they performed LES using the Smagorinsky subgrid scale model to predict the thermal and flow fields with and without the application of magnetic field. This strategy was further extended by Jung *et al.*[163] in their study on thermal, flow, and oxygen distributions in the Si-CZ growth process.

Cen *et al.*[164] performed LES and studied the damping of melt convection and temperature fluctuations with magnetic field (in vertical and cusp configurations) and without magnetic field. Liu *et al.*[165] carried out LES of melt turbulence for a 300-mm CZ-Si crystal growth using a dynamic Smagorinsky subgrid scale model. Liu *et al.*[166] studied the effect of cusp-shaped magnetic field (different type and strength) on the melt convection and oxygen transport in an industrial CZ crystal growth using a low-*Re* k–ε model, whereas Zhou and Huang[167] performed similar studies with rotating magnetic field again using a low-*Re* k–ε turbulence model. Fang *et al.*[168] compared several CZ furnace designs with different furnace enclosures with respect to the suppression of 3D effects for achieving axisymmetric flow pattern and temperature distribution in a CZ setup using the standard k–ε model. Noghabi *et al.*[169] carried out 2D analysis in CZ melt to find out the heat transfer and melt flow conditions which result in a particular interface shape using a one-equation turbulence model based on the RANS approach. Kirpo[170] carried out global simulation of CZ furnace and developed a self-consistent model that included turbulent heat and mass transports, oxygen transport, evolution of latent heat, and interface deflection using the commercial software FLUENT. His model predicted the effect of crucible rotation on the oxygen distribution in the crystal quite well; however, the predicted interface calculations were not satisfactory.

Having reviewed the studies on solidification with turbulence covering welding, casting and CZ crystal growth in the above three subsections, it is important to summarize the important findings and observations on different turbulence models/approaches regarding their applicability, accuracy, ease of computations, and limitations in modeling solidification with turbulence, and this is done in the following paragraphs.

RANS-Based Models: These models turn out to be first choice for a faster and easy to implement approach to tackle turbulence in a solidifying domain. There is a widespread applicability of the standard k–ε model in effectively capturing the turbulence in solidification problems as observed from the literature survey. These models have shown significant progress in modeling solidification with turbulence starting from the early mixing length models to the latest low-*Re* k–ε model. A no. of studies have demonstrated and validated the efficiency of these models in resolving large/macro scale turbulence phenomenon in solidification, which is adequate in some cases. However, due to the smearing effect of these models on the instantaneous fluctuations in flow properties, they fail to capture the microlevel effects and the anisotropies usually encountered in the mushy-zone modeling and near-wall damping. It is apparent that for a complete 3D modeling of convection a full time-dependent method should be employed, and as emphasized by Seidl *et al.*,[171] the steady-state RANS modeling may not be able to provide the desired accuracy in such cases. Also for a complete 3D model with RANS approach, the damping at the wall and at the solid–liquid interface is always difficult to model due to significant anisotropy of flow and the nonstationary wall treatment at the moving interface. All these factors point toward a higher level of modeling approach for solidification with turbulence.

LES: LES is the next level for modeling solidification with turbulence which handles most of the limitations of the RANS models at ease and effectively captures the subgrid scale effects at the microlevel and the flow anisotropy with a reasonably higher computational cost. The key to a successful LES study is the choice of suitable subgrid scale (SGS) model. A careful selection for an SGS model for solidification phenomena should ensure that the geometry, damping at walls and at interface, dynamics of the domain, vorticity effects, *etc.*, are fully captured. Standard SGS models, dynamic SGS models, LES/RANS hybridization or a standard SGS model with modifications to suit the physical domain to be modeled are frequently employed as seen from the literature review. It should be highlighted that the level of difficulty can be reduced only by increasing the understanding of the physics of the problem, the SGS model, and the numerical approach as LES models are highly sensitive to errors in modeling, numerics, and also to the treatment of boundary condition because of possible nonlinear interaction between the SGS modeling errors and numerical errors over time leading to unpredictable and impractical results. Also sufficient care has to be taken in the near-wall region with regard to the turbulent boundary layer as highlighted by Larsson and Kawai.[172] As far as the selection of an SGS model is concerned, the standard Smagorinsky model which is simple, robust, and computationally inexpensive has been employed in most of studies. Recently, the use of one-equation SGS models and the dynamic SGS models have started, guided by the evolutionary study of Germano.[160,173] LES studies on solidification are limited, but still they have shown considerable refinement in the recent past with regard to the SGS modeling.

DNS: DNS is the highest level for modeling solidification with turbulence, and it fully resolves all the length and time scales. However, a high computational cost involved restricts its applicability to idealized cases with simple geometries. Still, the qualitative and quantitative information generated in a DNS study is vital for the validation of both the LES and the RANS-based models for modeling solidification as is evident from the literature review presented here.

General comments: As we moved from modeling of welding to casting and then finally to the modeling of CZ crystal growth, the no. of studies as well as the complexity of the model has increased significantly. To the best of the authors knowledge, only one study using LES in welding has been reported in the literature, and this increased to a few studies in case of modeling casting process and finally a large no. of studies have been reported in the literature using LES in case of CZ crystal growth. We have also observed that the sophistication level of LES studies also increased in a similar manner. A similar trend is also observed for DNS studies. We could not find any DNS study on welding and casting, while quite a good no. of studies using DNS in case of CZ crystal growth have been reported in the literature. However, this observation does neither undermine the significant modeling study done in the area of welding and casting nor does it compare the model complexities for the three processes. The idea is to highlight the importance of microlevel defects in overall performance of single crystal material in electronic and optoelectronic devices, functionality of which depends on the perfection in a material up to lattice spacing (~Å level) and clearly justifies the need for a DNS study in case of modeling growth of single crystals.

VIII. IMPORTANT BENCHMARKING WORKS

The validation of a developed model is an important step to ensure that it possesses the necessary physics of the problem. The developed model can be validated by a similar simplified problem analytical solution of which exists. If the model under consideration has complexity in mathematics and physical configuration and the corresponding analytic solutions for the purpose of the validation are not available, then a similar experimental result or a similar numerical result with specified accuracy and exactness of the proposed solution in accordance with some specified grid convergence and reproducibility can also be used as a benchmark to validate the mathematical model. For the case of solidification modeling, the benchmarking results are classified into two major categories, namely, benchmarking results for the solidification of pure metals, and benchmarking results for the alloy solidification. The important results under these two categories are discussed below.

A. *Benchmarking Results for Solidification of Pure Metal*

Initial analytical solutions to 1D heat conduction involving change of state for a pure metal were provided by Carslaw and Jaeger.[174] Later, Dantzig and Rappaz[175] have provided an analytical solution to the 1D solidification of a pure metal in a mold which provides the temperature distribution and interface position at different solidification times. As far as the experimental benchmarking results for the pure metal solidification are concerned, the most commonly cited study is that of Wolff and Viskanta[45] who experimentally measured the solid–liquid interface positions at different time intervals during the solidification of the molten tin. Another widely cited work is that of Gau and Viskanta[176] who measured the position of the phase-change boundary as well as the temperature distribution and temperature fluctuations during the melting, and the solidification of pure gallium in a rectangular cell. Using this as the qualitative information, they predicted the natural convection flow structures in the melt during the phase change. However, the flow structure predicted is a point of controversy since Dantzig[177] reported a multicellular flow structure in the liquid region in contrast to a single-cell flow structure predicted by them. Later, Hannoun *et al.*[178] have tried to resolve this controversy by carrying out a systematic study with different grid sizes and discretization schemes of different orders.

B. *Benchmarking Results for Alloy Solidification*

Carlaw and Jaeger[174] also provided analytic solutions to 1D heat conduction involving change of state for an alloy. Later, Dantzig and Rappaz[175] have provided analytical solutions to 1D planar front solidification of a binary alloy and transient solidification of a binary alloy at a constant velocity. Important experimental benchmarks are the studies of Hebditch and Hunt[179] who experimentally studied the progress of macrosegregation and determined the concentration distribution and shape and location of the interface at a given stage of freezing using the quenching technique for Pb-48 pct Sn, Sn-5 pct Pb, and Sn-5 pct Zn alloys. Their macrosegregation experiment is frequently referenced and used to validate model predictions by many researchers. Another important benchmark is study by Beckermann and Viskanta[75] on the visualization of convection and solidification phenomena for ammonium chloride-water (NH_4Cl-H_2O) solution in an insulated test cell of a square cross section. Ammonium chloride is frequently used as a metal analog to carry out model experiments for the alloy solidification. This is due to its transparent and phase-change characteristics similar to those of metals and alloys. Further, the melting point of ammonium chloride is lower than that of metals; therefore, *in situ* measurements of growth characteristics can be carried out at room temperature under a microscope. Krane and Incropera[180] carried out solidification experiments for binary metal alloys, such as Pb-20 pct Sn and Pb-40 pct Sn in a mold. Bellet *et al.*[181] conducted an exercise to compare different physical models (with different numerical methods and algorithms) developed by various researchers for the solidification of Pb-18 pct Sn and Sn-10 pct Pb alloys in a 2D rectangular mold aiming at finding a numerical benchmark reference result for the binary alloy solidification. Similar study was earlier conducted by Gobin and Lequere[182] for a 2D solution of Tin melting from a vertical wall. Recently, Carozzani *et al.*[183] have reported a benchmark experiment for the solidification of Sn-3 pct Pb alloy and have performed a comparative study of the experimental results with the modeled results.

IX. CHALLENGES AND FUTURE DIRECTIONS

The challenges to effective and accurate modeling of solidification phenomena are manifold and arise due to different aspects related to the physics of the solidification phenomena, the accuracy, and the convergence of numerical techniques, nonavailability of correct material properties, paucity of reliable data for the validation, and lastly due to the limitations of the computational resource to carry out a complete direct numerical simulation for a general solidification problem.

Solidification modeling forms a specialized field in the continuum-modeling domain, and it requires enough proficiency to handle the physical and the numerical solution parts of the problem at hand. For the physical part, the complexities of the physics of solidification have been discussed to some extent in the current article and modeling such phenomena requires amalgamation of thermodynamics, fluid flow, heat and mass transfers, microstructure prediction, segregation effects, and chemical reactions in some cases. Further, as far as the numerical part is concerned, a selection of an appropriate grid size, discretization schemes, and specialized solidification models is extremely important. Choice of lower-order scheme may introduce inaccuracy in the solution, while a higher-order scheme introduces oscillations in the solution and may lead to divergence.

Specification of accurate material properties, specifying their anisotropy and correct dependency on temperature, pressure, *etc*., is indispensible as solidification phenomena encounter microscopic effects. Even a small level of under or overprediction at the microscopic level may induce significant errors to the solution at the continuum level. The dearth of reliable phase diagrams and high-quality thermodynamic data bank adds to the existing complexities.

However, the most important requirement is the modeling and quantification of defects during the solidification and the need to calculate the optimized solidification conditions in a backward manner as highlighted by many authors.[21,184,185] It is extremely important that solidification models incorporate nonequilibrium aspects as highlighted by Barbosa[186] and have a precise microscale to macroscale coupling.[6,131,187] Fisher *et al*.[188] have highlighted the need for soft computing techniques, such as genetic algorithms for the optimization of a process model. Genetic algorithms would automatically solve complex tasks involving geometry optimization, flow pattern modification (with the application of external force for example magnetic field, *etc*.,) and automatic selection of materials.

An estimate by Voller and Porte-Agel[189] suggests that a direct numerical simulation for casting with a domain length scale of 1 m and with grid resolution length scale up to 1 μm, (dendritic spacing) would be possible only by the year 2055, and if we go down to the lattice spacing resolution (1 nm) it would happen only in the year 2100. However, this time can be reduced to some extent by employing adaptive meshing techniques[190] and adopting a hybrid approach to solidification modeling.[191] Therefore, the future call is for an advancement in the multiscale/multiphysics hybrid models combining the continuum modeling to micro scale methods (such as the phase field modeling[192,193] and Lattice Boltzmann technique[191]), soft computing techniques (such as genetic algorithms[188]), and Monte Carlo methods and cellular automata models.[189] Asta *et al*.[187] have emphasized on the integration of molecular dynamics, phase-field technique and the recently developed phase-field crystal (PFC) method for a more realistic prediction of a real solidification process. It is also important to mention the future LES models in modeling solidification. The literature review clearly indicated that LES with dynamic SGS incorporating greater physics of the problem will support the solidification modeling requirements in the near future.

An increase in the predictive capability of a model is not worth without an equivalent benchmarking for the validation of its efficiency. Therefore, futuristic solidification modeling and sophisticated experimentation should also go hand in hand. For the realization of hybrid-modeling approach, a sophisticated experimental research yielding structural and chemical information with ultrahigh resolution is indispensible. Experimental support facilities like 3D imaging techniques and real-time *in situ* observation of dynamic evolution of solid–liquid interface during solidification will aid in getting deeper insight into the complex phenomena of solidification and defect formation.

X. CONCLUSIONS

In the modern-day world, numerical modeling has proven to be an indispensible tool aiding frontiers of industry, research, and academics. Numerical modeling has now become an essential part of various process optimizations including processes involving solidification. In the current article, different aspects and approaches related to the modeling of the solidification phenomena have been reviewed in a chronological order, to highlight the step- by step- advancement in the solidification modeling. Different formulations of the solidification modeling have been presented, highlighting their merits and demerits. Some of the approaches, such as the single-domain continuum formulation using the enthalpy–porosity approach and the mixture theory model for the alloy solidification, have been discussed in detail owing to their widespread applicability in modeling many solidification processes including welding, casting, and Czochralski crystal growth. As discussed in the current article, an important effect distinguishing solidification phenomena is welding, casting, and Czochralski crystal growth from other solidification processes is the presence of turbulence. Incorporation of turbulence modeling in solidification has been an area of extensive research, and the employment of RANS-based turbulence models, such as the standard k–ε model is now widespread in the modeling of these important processes. The importance of the low-Re k–ε model and its significance in these processes have also been discussed in the current article. It was observed that although RANS-based models dominated

the solidification modeling research, LES is rapidly emerging as an accurate and powerful tool in the solidification modeling of processes having turbulence. The importance of subgrid scale models in LES and the important issues with LES have also been discussed in the current article. However, as pointed out in the current article, a direct numerical simulation of the solidification process is still limited by the lack of computational resources to tackle the solidification process in its full-length and time scales. The use of multiscale/multiphysics hybrid models is seen as an important alternate to direct numerical simulation. A review of different benchmarking works clearly highlighted the dearth of model validation benchmarks. Therefore, the need for generating high-quality experimental and numerical benchmarking results is also highlighted in the current article.

We have presented an overview of a few important and emerging aspects of the solidification modeling among the countless research activities currently underway in this field. The importance of solidification modeling in dealing with a variety of problems has been highlighted. The importance of the solidification modeling will be significantly increasing with an increasing demand for the development of high-quality material using various solidification processes.

REFERENCES

1. W. Kurz and D.J. Fisher: *Fundamentals of Solidification*, 3rd ed., Trans Tech Publications Ltd, Dürnten, 1992.
2. *In-situ Studies with Photons, Neutrons and Electron Scattering*, 3rd ed., T. Kannengiesser, and S.S. Babu, and Y. Komizo, and A.J. Ramirez, eds., *In-situ Studies with Photons, Neutrons and Electron Scattering*, Springer, Berlin, 2010.
3. A. Clarke, S. Imhoff, P. Gibbs, J. Cooley, C. Morris, F. Merrill, B. Hollander, F. Mariam, T. Ott, M. Barker, T. Tucker, W. Lee, K. Fezzaa, A. Deriy, B. Patterson, K. Clarke, J. Montalvo, R. Field, D. Thoma, J. Smith and D. Teter: *Proton Radiography Peers into Metal Solidification*, Scientific Reports, Nature Publishing Group, Jun 19, 2013.
4. R.H. Mathiesen, L. Arnberg, K. Ramsøskar, T. Weitkamp, C. Rau, and A. Snigirev: *Metall. Mater. Trans. B*, 2002, vol. 33B, pp. 613–23.
5. P. Delaleau, R.H. Mathiesen, P.L. Schaffer, L. Arnberg, and C. Beckermann: in *Modeling of Casting, Welding and Advanced Solidification Processes-XII*, S.L. Cockcroft and D.M. Maijer, eds., TMS, Warrendale, 2009, pp. 643–50.
6. M. Rappaz: *Int. Mater. Rev.*, 1989, vol. 34 (3), pp. 93–123.
7. D. A. Drew: *Annu. Rev. Fluid Mech.*, 1983, vol. 13, pp. 261–91.
8. B. Basu and A.W. Date: *Sadhana*, 1988, vol. 13 (3), pp. 169–213.
9. H.E. Huppert: *J. Fluid Mech.*, 1990, vol. 212, pp. 209–40.
10. C. Beckermann and R. Viskanta: *Appl. Mech. Rev.*, 1993, vol. 46 (1), pp. 1–27.
11. H. Hu and S.A. Argyropoulos: *Model. Simul. Mater. Sci. Eng.*, 1996, vol. 4, pp. 371–96.
12. M.G. Worester: *Annu. Rev. Fluid Mech.*, 1997, vol. 29, pp. 91–122.
13. B.G. Thomas and L. Zhang: *ISIJ Int.*, 2001, vol. 41 (10), pp. 1181–93.
14. C. Beckermann: *Int. Mater. Rev.*, 2002, vol. 47 (5), pp. 243–61.
15. C.W. Lan: *Chem. Eng. Sci.*, 2004, vol. 59 (7), pp. 1437–57.
16. D. Apelian, H. Brody, and D. Backman: in *Modeling of Casting, Welding and Advanced Solidification Processes-XI*, C.A. Gandin and M. Bellet, eds., TMS, Warrendale, 2006, pp. 1–12.
17. C. Beckermann and C.Y. Wang: in *Annual Review of Heat Transfer VI*, C.L. Tien and B. House, eds., Begell House, New York, 1995, vol. 6, pp. 115–98.
18. *Continuum Scale Simulation of Engineering Materials: Fundamentals–Microstructures–Process Applications*, 3rd ed., D. Raabe, and F. Roters, and F. Barlat, and L. Chen, eds., *Continuum Scale Simulation of Engineering Materials: Fundamentals–Microstructures–Process Applications*, Wiley-VCH, Weinheim, 2004.
19. A.S. Jordan, R. Caruso, and A.R. Von Neida: *Bell Syst. Tech. J.*, 1980, vol. 59 (4), pp. 593–637.
20. N. Banos, J. Friedrich, and G. Muller: *J. Cryst. Growth*, 2008, vol. 310 (2), pp. 501–07.
21. G. Muller and J. Friedrich: *J. Cryst. Growth*, 2004, vol. 266 (1–3), pp. 1–19.
22. L.C. Wurker, M. Fackeldey, P.R. Sahm, and B.G. Thomas: in *Modeling of Casting, Welding and Advanced Solidification Processes-VIII*, B.G. Thomas and C. Beckermann, eds., TMS, Warrendale, 1998, pp. 795–802.
23. N. Chvorinov: *Giesserei*, 1940, vol. 27, pp. 177–80, 201–08, 222–25.
24. J. Campbell: *Casting*, 2nd ed., Elsevier Butterworth Heinemann, Oxford, 2003.
25. J. Campbell: *Castings Practice: The Ten Rules of Castings*, Elsevier Butterworth Heinemann, Oxford, 2004.
26. N.R. Eyres, D.R. Hartree, J. Ingham, R. Jackson, R.J. Sarjant, and S.M. Wagstaff: *Philos. Trans. R. Soc.*, 1946, vol. A240, pp. 1–57.
27. B. Chalmers: *Principles of Solidification*, Wiley, New York, 1964.
28. M.C. Flemings: *Solidification Processing*, McGraw-Hill, New York, 1974.
29. J. Crank: *Free and Moving Boundary Problems*, Clarendon Press, Oxford, 1984.
30. J. Szekely and V. Stanek: *Metall. Trans.*, 1970, vol. 1 (8), pp. 2243–51.
31. J. Szekely and P.C. Chabra: *Metall. Trans.*, 1970, vol. 1 (5), pp. 1195–1203.
32. R. Mehrabian, M. Keane, and M.C. Flemings: *Metall. Trans.*, 1970, vol. 1 (5), pp. 1209–20.
33. S.D. Ridder, S. Kou, and R. Mehrabian: *Metall. Trans. B*, 1981, vol. 12B, pp. 435–47.
34. R.N. Hills, D.E. Loper, and P.H. Roberts: *Q. J. Mech. Appl. Math.*, 1983, vol. 36 (4), pp. 505–40.
35. S.V. Patankar: *Numerical Heat Transfer and Fluid Flow*, McGraw-Hill, New York, 1980.
36. D.D. Gray and A. Giorgini: *Int. J. Heat Mass Transf.*, 1976, vol. 19 (5), pp. 545–51.
37. J. Stefan: *Sitzungsber. Oesterr. Akad. Math. Nat. Sci. Kl. Dept. 2*, 1889, vol. 98, pp. 473–84.
38. J. Stefan: *Wiedemann Ann. Phys. Chem.*, 1891, vol. 42, pp. 269–86.
39. V. Alexiades and A.D. Solomon: *Mathematical Modeling of Melting and Freezing Processes*, Hemisphere Publishing Corporation, Washington, DC, 1993.
40. S.C. Gupta: *The Classical Stefan Problem: Basic Concepts, Modelling and Analysis*, Elsevier, Amsterdam, 2003.
41. C. Bonacina, G. Comini, A. Fasano, and M. Primicerio: *Int. J. Heat Mass Transf.*, 1973, vol. 16 (10), pp. 1825–32.
42. C. Gau and R. Viskanta: *Int. J. Heat Mass Transf.*, 1984, vol. 27 (1), pp. 113–23.
43. E.M. Sparrow, S.V. Patankar, and S. Ramdhyani: *J. Heat Transf.*, 1977, vol. 99 (4), pp. 520–26.
44. N. Ramachandran and J.P. Gupta: *Int. J. Heat Mass Transf.*, 1982, vol. 25 (2), pp. 187–94.
45. F. Wolff and R. Viskanta: *Int. J. Heat Mass Transf.*, 1988, vol. 31 (8), pp. 1735–44.
46. S. Jana, S. Ray, and F. Durst: *Appl. Math. Model.*, 2007, vol. 31 (1), pp. 93–119.
47. I. Demirdzic and M. Peric: *Int. J. Numer. Methods Fluids*, 1990, vol. 10 (7), pp. 771–90.
48. I. Demirdzic and M. Peric: *Int. J. Numer. Methods Fluids*, 1988, vol. 8 (9), pp. 1037–50.
49. P.D. Thomas and C.K. Lombard: *AIAA J.*, 1979, vol. 17 (10), pp. 1030–37.
50. J.H. Ferziger and M. Peric: *Computational Methods for Fluid Dynamics*, 3rd ed., Springer, New York, 2002.
51. J. Szimmat: *Heat Mass Transf.*, 2002, vol. 38, pp. 279–93.
52. P.H. Price and M.R. Slack: *Br. J. Appl. Phys.*, 1954, vol. 5 (8), pp. 285–87.

53. V.R. Voller and M. Cross: *Int. J. Heat Mass Transf.*, 1981, vol. 24, pp. 545–56.
54. V.R. Voller, N.C. Markatos, and M. Cross: in *Numerical Simulations of Fluid Flow and Heat/Mass Transfer Processes*, N.C. Markatos, D.G. Tatchell, M. Cross, and N. Rhodes, eds., Springer, Berlin, 1996.
55. V.R. Voller, N.C. Markatos, and M. Cross: in *Numerical Methods in Thermal Problems*, R.W. Lewis and K. Morgan, eds., Pineridge Press, Swansea, 1985.
56. V.R. Voller, M. Cross, and N.C. Markatos: *Int. J. Numer. Methods Eng.*, 1987, vol. 24, pp. 271–84.
57. A.D. Brent, V.R. Voller, and K.J. Reid: *Numer. Heat Transf.*, 1988, vol. 13 (3), pp. 297–318.
58. V.R. Voller and C. Prakash: *Int. J. Heat Mass Transf.*, 1987, vol. 30 (8), pp. 1709–19.
59. K. Morgan: *Comput. Methods Appl. Mech. Eng.*, 1981, vol. 28 (3), pp. 275–84.
60. D.K. Gartling: in *Computer Methods in Fluids*, K. Morgan, C. Taylor, and C.A. Brebbia, eds., Pentech, London, 1980.
61. D. R. Poirier: *Metall. Trans. B*, 1987, vol. 18B, pp. 245–55.
62. A.K. Singh, R. Pardeshi, and B. Basu: *Sadhana*, 2001, vol. 26 (Parts 1 & 2), pp. 139–62.
63. C.R. Swaminathan and V.R. Voller: *Metall. Trans. B*, 1992, vol. 23B (5), pp. 651–64.
64. C.R. Swaminathan and V.R. Voller: *Int. J. Numer. Methods Heat Fluid Flow*, 1993, vol. 3 (3), pp. 233–44.
65. V.R. Voller, C.R. Swaminathan, and B.G. Thomas: *Int. J. Numer. Methods Eng.*, 1990, vol. 30 (4), pp. 875–98.
66. M.C. Flemings and G.E. Nereo: *Trans. TMS-AIME*, 1967, vol. 239, pp. 1449–61.
67. M.C. Flemings, R. Mehrabian, and G.E. Nereo: *Trans. TMS-AIME*, 1968, vol. 242, pp. 41–49.
68. M.C. Flemings and G.E. Nereo: *Trans. TMS-AIME*, 1968, vol. 242, pp. 50–55.
69. J. Szekely and A.S. Jassal: *Metall. Trans. B*, 1978, vol. 9B, pp. 389–98.
70. T. Fuji, D.R. Poirier, and M.C. Flemings: *Metall. Trans. B*, 1979, vol. 10B, pp. 331–39.
71. V.C. Prantil and P.R. Dawson: in *Transport Phenomena in Materials Processing*, M.M. Chen, J. Mazumder, and C.L. Tucker, III, eds., ASME, New York, 1983, pp. 469–84.
72. J.S. Turner: *Annu. Rev. Fluid Mech.*, 1974, vol. 6, pp. 37–54.
73. J.S. Turner: *Buoyancy Effects in Fluids*, Cambridge University Press, Cambridge, 1979.
74. H.E. Huppert and J.S. Turner: *J. Fluid Mech.*, 1981, vol. 106, pp. 299–329.
75. C. Beckermann and R. Viskanta: *PCH, PhysicoChem. Hydrodyn.*, 1988, vol. 10 (2), pp. 195–213.
76. C. Beckermann and R. Viskanta: *Int. J. Heat Mass Transf.*, 1988, vol. 31 (10), pp. 2077–89.
77. B. Basu and A.K. Singh: *Proceedings of the 3rd ISHMT-ASME Heat and Mass Transfer Conference and 14th National Heat and Mass Transfer Conference*, IIT, Kanpur, 1997, pp. 129–61.
78. W.D. Bennon and F.P. Incropera: *Int. J. Heat Mass Transf.*, 1987, vol. 30 (10), pp. 2161–70.
79. W.D. Bennon and F.P. Incropera: *Int. J. Heat Mass Transf.*, 1987, vol. 30 (10), pp. 2171–87.
80. J. Ni and C. Beckermann: *Metall. Trans. B*, 1991, vol. 22B, pp. 349–61.
81. I.A. Muller: *Arch. Ration. Mech. Anal.*, 1968, vol. 28 (1), pp. 1–39.
82. R.M. Bowen: *Arch. Ration. Mech. Anal.*, 1967, vol. 24 (5), pp. 370–403.
83. W.T. Sha and S.L. Soo: *Int. J. Heat Mass Transf.*, 1978, vol. 21 (12), pp. 1581–95.
84. D.S. Drumheller: *Int. J. Solids Struct.*, 1978, vol. 14 (6), pp. 441–56.
85. J.W. Nunziato: *Theory of Dispersed Multiphase Flow*, Academic Press, New York, 1983, pp. 191–226.
86. V.R. Voller, A.D. Brent, and C. Prakash: *Int. J. Heat Mass Transf.*, 1989, vol. 32 (9), pp. 1719–31.
87. M. Hassanizadeh and W.G. Gray: *Adv. Water Resour.*, 1990, vol. 13 (4), pp. 169–86.
88. D.A. Drew and S.L. Passman: *Theory of Multicomponent Fluids*, Springer, New York, 1999.
89. W.G. Gray: *Chem. Eng. Sci.*, 1975, vol. 30 (2), pp. 229–33.
90. W.G. Gray: *Adv. Water Resour.*, 1983, vol. 6 (3), pp. 130–40.
91. M. Hassanizadeh and W.G. Gray: *Adv. Water Resour.*, 1979, vol. 2, pp. 131–44.
92. M. Hassanizadeh and W.G. Gray: *Adv. Water Resour.*, 1979, vol. 2, pp. 191–203.
93. M. Hassanizadeh and W.G. Gray: *Adv. Water Resour.*, 1980, vol. 3 (1), pp. 25–40.
94. S. Ganesan and D.R. Poirier: *Metall. Trans. B*, 1990, vol. 21B, pp. 173–81.
95. C. Prakash: *Numer. Heat Transf. B*, 1990, vol. 18 (2), pp. 131–45.
96. C. Prakash: *Numer. Heat Transf. B*, 1990, vol. 18 (2), pp. 147–67.
97. P.J. Prescott, F.P. Incropera, and W.D. Bennon: *Int. J. Heat Mass Transf.*, 1991, vol. 34 (9), pp. 2351–59.
98. J. Ni and F.P. Incropera: *Int. J. Heat Mass Transf.*, 1995, vol. 38 (7), pp. 1271–84.
99. J. Ni and F.P. Incropera: *Int. J. Heat Mass Transf.*, 1995, vol. 38 (7), pp. 1285–96.
100. A.V. Reddy and C. Beckermann: *Metall. Mater. Trans. B*, 1997, vol. 28B, pp. 479–89.
101. M.J.M. Krane, F.P. Incropera, and D.R. Gaskell: *Int. J. Heat Mass Transf.*, 1997, vol. 40, pp. 3828–35.
102. M.J.M. Krane and F.P. Incropera: *Int. J. Heat Mass Transf.*, 1997, vol. 40, pp. 3837–47.
103. I. Vusanovi, B. Sarler, and M.J.M. Krane: *Mater. Sci. Eng. A*, 2005, vols. 413–414, pp. 217–22.
104. M.J.M. Krane, F.P. Incropera, and D.R. Gaskell: *Metall. Mater. Trans. A*, 1998, vol. 29A, pp. 843–53.
105. S.A. Cefalu and M.J.M. Krane: *Mater. Sci. Eng. A*, 2007, vols. 454–455, pp. 371–78.
106. A. Dewan: *Tackling Turbulent Flows in Engineering*, Springer, New York, 2011.
107. T. Zacharia, A.H. Eraslan, and D.K. Aidun: *Weld. J.*, 1988, vol. 67, pp. 53s–62s.
108. K. Mundra, T. Debroy, T. Zacharia, and S.A. David: *Weld. J.*, 1992, vol. 71, pp. 313s–20s.
109. R.T.C. Choo and J. Szekely: *Weld. J.*, 1994, vol. 73, pp. 25–31.
110. N. Chakraborty, S. Chakraborty, and P. Dutta: *Int. J. Numer. Methods Heat Fluid Flow*, 2003, vol. 13 (1), pp. 7–30.
111. N. Chakraborty, S. Chakraborty, and P. Dutta: *Numer. Heat Transf. A*, 2004, vol. 45, pp. 391–413.
112. N. Chakraborty and S. Chakraborty: *Int. J. Heat Mass Transf.*, 2007, vol. 50, pp. 1805–22.
113. K. Abderrazak, W.B. Salem, H. Mhiri, G. Lepalec, and M. Autric: *Opt. Laser Technol.*, 2008, vol. 40, pp. 581–88.
114. N. Chakraborty: *Appl. Therm. Eng.*, 2009, vol. 29, pp. 3618–31.
115. D. Chatterjee and S. Chakraborty: *Metall. Mater. Trans. B*, 2005, vol. 36B, pp. 743–54.
116. S. Asai and J. Szekely: *Ironmak. Steelmak*, 1975, vol. 3, pp. 205–13.
117. W. Shyy, Y. Pang, D.Y. Wei and M.H. Chen: AIAA 28th Aerospace Science Meeting, Paper number 91-0506, 1991.
118. A. Murthy, J. Szekely, and N. El-Kaddah: *Metall. Trans. B*, 1988, vol. 19B, pp. 765–75.
119. B.E. Launder and D.B. Spalding: *Comput. Methods Appl. Mech. Eng.*, 1974, vol. 3, pp. 269–89.
120. B.G. Thomas, L.J. Mika, and F.M. Nazzar: *Metall. Trans. B*, 1990, vol. 21B, pp. 387–400.
121. P.J. Flint: *Steelmaking Conference Proceedings*, 1990, pp. 481–90.
122. X. Huang, B.G. Thomas, and F.M. Nazzar: *Metall. Trans. B*, 1992, vol. 23B, pp. 339–56.
123. B.Q. Li: *J. Mater. Process. Technol.*, 1995, vol. 55 (3–4), pp. 351–59.
124. W. Shyy, Y. Pang, G.B. Hunter, D.Y. Wei, and M.H. Chen: *Int. J. Heat Mass Transf.*, 1992, vol. 35 (5), pp. 1229–45.
125. B. Farouk, D. Apelian, and Y.G. Kim: *Metall. Trans. B*, 1992, vol. 23B, pp. 477–92.
126. H. Murakami: Ph.D. Thesis, Department of Mining and Metallurgical Engineering, McGill University, 1993.
127. M.R. Aboutalebi, M. Hasan, and R.I.L. Guthrie: *Metall. Mater. Trans. B*, 1995, vol. 26B, pp. 731–44.
128. S.H. Seyedein and M. Hasan: *Int. J. Heat Mass Transf.*, 1997, vol. 40 (18), pp. 4405–23.
129. R.I.L. Guthrie and R.P. Tavares: *Appl. Math. Model.*, 1998, vol. 22 (11), pp. 851–72.

130. P.Q.G. Netto and R.I.L. Guthrie: *Int. J. Heat Mass Transf.*, 2000, vol. 43 (1), pp. 21–37.
131. S. Chakraborty, N. Chakraborty, P. Kumar, and P. Dutta: *Int. J. Heat Mass Transf.*, 2003, vol. 46 (7), pp. 1115–37.
132. B. Zhao, B.G. Thomas, S.P. Vanka, and R.J. O'malley: *Metall. Mater. Trans. B*, 2005, vol. 36B, pp. 801–23.
133. C. Ji, J. Li, S. Yang, and L. Sun: *J. Iron Steel Res. Int.*, 2013, vol. 20(1), pp. 34–39, 46.
134. Q. Yuan and B.G. Thomas: in *Modeling of Casting, Welding and Advanced Solidification Processes-XI*, C.A. Gandin and M. Bellet, eds., TMS, Warrendale, 2006, pp. 745–52.
135. Q. Yuan, S.P. Vanka and B.G. Thomas: *Proceeding of 3rd International Symposium on Turbulence and Shear Flow Phenomena*, Sendai, 2003, vol. 2, pp. 681–86.
136. R. Chaudhary, B.G. Thomas, and S.P. Vanka: *Metall. Mater. Trans. B*, 2012, vol. 43B, pp. 532–53.
137. P. Sagaut: *Large Eddy Simulation for Incompressible Flows*, 2nd ed., Springer, New York, 2002.
138. *Bulk Crystal Growth of Electronic, Optical and Optoelectronic Materials*, 2nd ed., P. Capper, ed., *Bulk Crystal Growth of Electronic, Optical and Optoelectronic Materials*, Wiley, London, 2005.
139. J.R. Ristorcelli and J.L. Lumley: *J. Cryst. Growth*, 1992, vol. 116, pp. 447–60.
140. S. Kobayashi, S. Miyahara, T. Fujiwara, T. Kubo, and H. Fujiwara: *J. Cryst. Growth*, 1991, vol. 109 (1–4), pp. 149–54.
141. J.R. Ristorcelli and J.L. Lumley: *J. Cryst. Growth*, 1993, vol. 129 (1–2), pp. 249–65.
142. R. Assaker, N. Van den Bogaert, and F. Dupret: *J. Cryst. Growth*, 1997, vol. 180 (3–4), pp. 450–60.
143. A. Lipchin and R.A. Brown: *J. Cryst. Growth*, 1999, vol. 205 (1–2), pp. 71–91.
144. B. Basu, S. Enger, M. Breuer, and F. Durst: *J. Cryst. Growth*, 2000, vol. 219 (1–2), pp. 123–43.
145. S. Enger, B. Basu, M. Breuer, and F. Durst: *J. Cryst. Growth*, 2000, vol. 219 (1–2), pp. 144–64.
146. S. Enger, O. Grabner, G. Muller, M. Breuer, and F. Durst: *J. Cryst. Growth*, 2001, vol. 230 (1–2), pp. 135–42.
147. D. Vizman, O. Grabner, and G. Muller: *J. Cryst. Growth*, 2001, vol. 233 (4), pp. 687–98.
148. D. Vizman, J. Friedrich, and G. Muller: *J. Cryst. Growth*, 2001, vol. 230 (1–2), pp. 73–80.
149. I.Y. Evstratov, V.V. Kalaev, A.I. Zhmakin, Y.N. Makarov, A.G. Abramov, N.G. Ivanov, A.B. Korsakov, E.M. Smirnov, E. Dornberger, J. Virbulis, E. Tomzig, and W. von Ammon: *J. Cryst. Growth*, 2002, vols. 237–239 (part 3), pp. 1757–61.
150. N.G. Ivanov, A.B. Korsakov, E.M. Smirnov, K.V. Khodosevitch, V.V. Kalaev, Y.N. Makarov, E. Dornberger, J. Virbulis, and W. von Ammon: *J. Cryst. Growth*, 2003, vol. 250 (1–2), pp. 183–88.
151. V.V. Kalaev, I.Y. Evstratov, and Y.N. Makarov: *J. Cryst. Growth*, 2003, vol. 249 (1–2), pp. 87–99.
152. A. Krauze, A. Muiznieks, A. Muhlbauer, T. Wetzel, and W. Ammon: *J. Cryst. Growth*, 2004, vol. 262 (1–4), pp. 157–67.
153. C. Wagner and R. Friedrich: *Int. J. Heat Mass Transf.*, 2004, vol. 25 (3), pp. 431–43.
154. O.V. Smirnova, V.V. Kalaev, Y.N. Makarov, N.V. Abrosimov, and H. Riemann: *J. Cryst. Growth*, 2006, vol. 287 (2), pp. 281–86.
155. S. Son, P. Nam, and K. Yi: *J. Cryst. Growth*, 2006, vol. 292 (2), pp. 272–81.
156. A. Raufeisen, M. Breuer, T. Botsch, and A. Delgado: *Int. J. Heat Mass Transf.*, 2008, vol. 51, pp. 6219–34.
157. A. Raufeisen, M. Breuer, T. Botsch, and A. Delgado: *Comput. Fluids*, 2009, vol. 38, pp. 1549–65.
158. A. Raufeisen, M. Breuer, T. Botsch, and A. Delgado: *J. Cryst. Growth*, 2009, vol. 311, pp. 695–97.
159. A. Raufeisen, M. Breuer, T. Botsch, and A. Delgado: *J. Cryst. Growth*, 2010, vol. 312 (16–17), pp. 2297–99.
160. M. Germano, U. Piomelli, P. Moin, and W.H. Cabot: *Phys. Fluids A*, 1991, vol. 3 (7), pp. 1760–65.
161. O.A. Noghabi, M. M'Hamdi, and M. Jomaa: *J. Cryst. Growth*, 2011, vol. 318 (1), pp. 173–77.
162. W. Miller, C. Frank-Rotsch, and P. Rudolph: *J. Cryst. Growth*, 2011, vol. 318 (1), pp. 244–48.
163. T. Jung, J. Seebeck, and J. Friedrich: *J. Cryst. Growth*, 2013, vol. 368, pp. 72–80.
164. X. Cen, Y.S. Li, and J. Zhan: *J. Cryst. Growth*, 2012, vol. 340 (1), pp. 135–41.
165. L. Liu, X. Liu, and Y. Wang: *Int. J. Heat Mass Transf.*, 2012, vol. 55, pp. 53–60.
166. X. Liu, L. Liu, Z. Li, and Y. Wang: *J. Cryst. Growth*, 2012, vol. 354 (1), pp. 101–08.
167. X. Zhou and H. Huang: *J. Cryst. Growth*, 2012, vol. 340 (1), pp. 166–70.
168. H.S. Fang, Z.L. Jin, and X.M. Huang: *J. Cryst. Growth*, 2012, vol. 361, pp. 114–20.
169. O.A. Noghabi, M. Jomaa, and M. M'hamdi: *J. Cryst. Growth*, 2013, vol. 362, pp. 77–82.
170. M. Kirpo: *J. Cryst. Growth*, 2013, vol. 371, pp. 60–66.
171. A. Seidl, G. Mueller, E. Dornberger, E. Tomzig, B. Rexer, and W. Ammon: in *Proceedings of the Eighth International Symposium on Silicon Materials Science and Technology*, H.R. Huff, U. Gosele, and H. Tsuya, eds., Electrochemical Society, Pennington, 1998, pp. 417–28.
172. J. Larsson and S. Kawai: *Annual Research Briefs*, Center for Turbulence Research, Stanford, 2010, pp. 39–46.
173. M. Germano: *J. Fluid Mech.*, 1992, vol. 238, pp. 325–36.
174. H.S. Carlaw and J.C. Jaeger: *Conduction of Heat in Solids*, 2nd ed., Oxford University Press, London, 1959.
175. J.A. Dantzig and M. Rappaz: *Solidification*, 1st ed., EPFL Press, Lausanne, 2009.
176. C. Gau and R. Viskanta: *J. Heat Transf.*, 1986, vol. 108 (1), pp. 174–81.
177. J.A. Dantzig: *Int. J. Numer. Methods Eng.*, 1989, vol. 28 (8), pp. 1769–85.
178. N. Hannoun, V. Alexiades, and T.Z. Mai: *Numer. Heat Transf. B*, 2003, vol. 44 (3), pp. 253–76.
179. D.J. Hebditch and J.D. Hunt: *Metall. Trans.*, 1974, vol. 5, pp. 1157–1564.
180. M.J.M. Krane and F.P. Incropera: *J. Heat Transf.*, 1997, vol. 119 (4), pp. 783–91.
181. M. Bellet, H. Combeau, Y. Fautrelle, D. Gobin, M. Rady, E. Arquis, O. Budenkova, B. Dussoubs, Y. Duterrail, A. Kumar, C. A. Gandin, B. Goyeau, S. Mosbah, and M. Zaloznik: *Int. J. Therm. Sci.*, 2009, vol. 48 (11), pp. 2013–16.
182. D. Gobin and P. Lequere: *Comput. Assist. Mech. Eng. Sci.*, 2000, vol. 7, pp. 289–306.
183. T. Carozzani, C. Gandin, H. Digonnet, M. Bellet, K. Zaidat, and Y. Fautrelle: *Metall. Mater. Trans. A*, 2013, vol. 44A, pp. 873–87.
184. G. Muller: *J. Cryst. Growth*, 2002, vols. 237–239 (3), pp. 1628–37.
185. C. Reilly, N.R. Green, and M.R. Jolly: *Appl. Math. Model.*, 2013, vol. 37 (3), pp. 611–28.
186. J.R. Barbosa: *J. Braz. Soc. Mech. Sci. Eng.*, 2005, vol. 27 (1), pp. 31–45.
187. M. Asta, C. Beckermann, A. Karma, W. Kurz, R. Napolitano, M. Plapp, G. Purdy, M. Rappaz, and R. Trivedi: *Acta Mater.*, 2009, vol. 57 (4), pp. 941–71.
188. B. Fischer, J. Friedrich, T. Jung, M. Hainke, J. Dagner, T. Fuhner, and P. Schwesig: *J. Cryst. Growth*, 2005, vol. 275 (1–2), pp. 240–50.
189. V.R. Voller and F. Porte-Agel: *J. Comput. Phys.*, 2002, vol. 179 (2), pp. 698–703.
190. N. Provatas, N. Goldenfeld, and J. Dantzig: *J. Comput. Phys.*, 1999, vol. 148, pp. 265–90.
191. D. Chatterjee and S. Chakraborty: *Phys. Lett. A*, 2006, vol. 351 (4–5), pp. 359–67.
192. F. Ferreira, L.O. Ferreira, and A.C. Assis: *J. Braz. Soc. Mech. Sci. Eng.*, 2011, vol. 33 (2), pp. 125–30.
193. W.J. Boettinger, J.A. Warren, C. Beckermann, and A. Karma: *Annu. Rev. Mater. Res.*, 2002, vol. 32, pp. 163–94.